CHAPTER 2

Removal of organic solvents through a fatty acid grafted polyvinyl alcohol based organogel

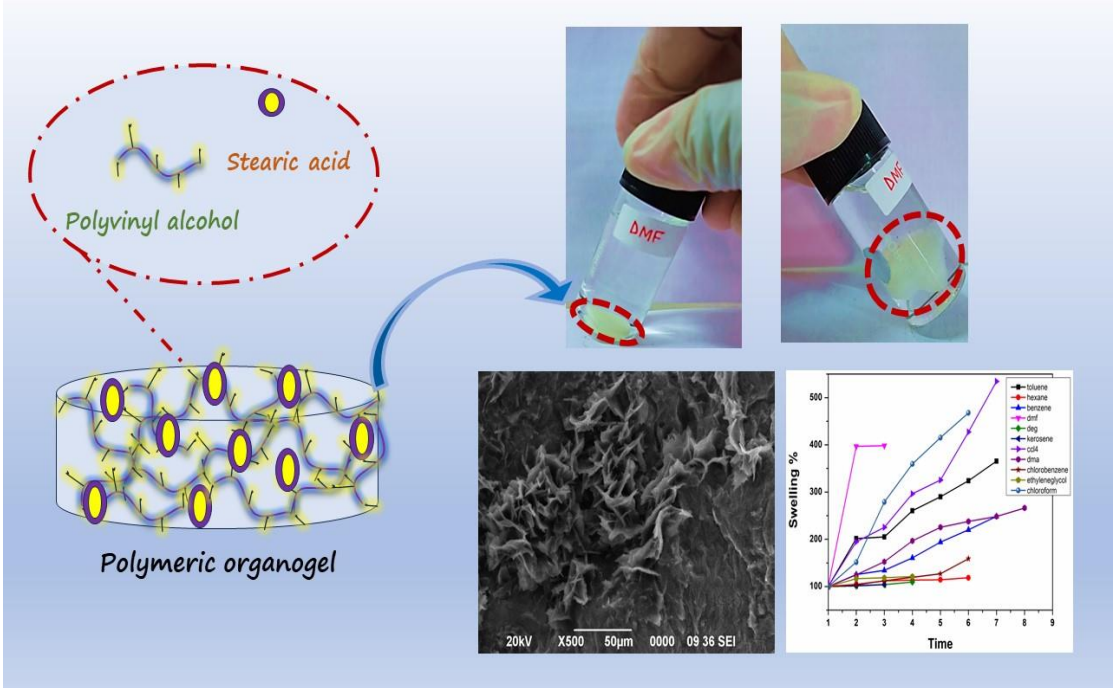

This chapter describes the formation of polymeric organogel and its application in solvent absorption

---

This part of the thesis is published in:

Baruah, K., Ahmed, A., Dutta, R., Ahmed, S., Lahkar, S., and Dolui, S.K. Removal of organic solvents from contaminated water surface through a fatty acid grafted polyvinyl alcohol (PVA) based organogel. ***Journal of Applied Polymer Science***, 139 (45), 2022.

2.1 INTRODUCTION

An alarming and appalling situation has arisen due to excessive human exploitation, posing a serious threat to the aquatic ecosystem [1]. Petroleum industries, in the course of manufacturing or transportation, are directly releasing oil seepages into the water system, resulting in the death of numerous aquatic species [2-5]. Industrial waste serves as a significant source of pollution, consisting of various organic and inorganic pollutants in both solid and liquid forms [5]. The hazardous liquid waste contains toxic pollutants such as pesticides [6], fluorinated compounds (FC) [7], phenols [8], chlorinated phenols [9,10], azo dyes [11,12], petroleum hydrocarbons [13,14], organic solvents [15,16], and toxic heavy metals [17,18], posing a serious threat to both human health and the environment [19]. These organic pollutants can be remediated through physical, chemical, and biological treatment methods. However, the physical method of 'sorbent' has been extensively used for the effective and excellent cleanup of pollutants from the water surface into a semi-solid phase/material [20–23].

Numerous materials have been employed for the selective absorption of solvents. Erden [24] successfully prepared a novel hydrophobic organogel using diamino-terminated polypropylene glycol and diphenylmethane bismaleimide for the successful recovery of organic solvents, achieving the highest absorbency of 729.60% for dichloromethane. Sar et al. [25] developed a crosslinked polymeric organogel using dimethyl 2-(methylacrylamido)pentanedioate (Glu-MAC) with pendant glutamate moieties, which exhibited a dye removal efficiency of 99%. Goel and Jacob [26] reported the formation of an organogel using acrylate-based linear and crosslinked polymers with D-galactose, capable of selectively adsorbing dyes and solvents, with a maximum swelling of 935% in chloroform. Bidgoli et al. [27] prepared an aerogel with high absorption and excellent oil selectivity by functionalizing cellulose with octanoyl chloride in an organic medium. Nguyen and colleagues [28] conducted a study on a cellulose/polyurethane composite that exhibits considerable oil absorption capabilities.

PVA, which is economically available and non-toxic [29–31], has been extensively studied for its absorbent properties by modifying its surface. For example, PVA/Cellulose nanofiber aerogels modified with MTMS have shown excellent oil/solvent sorption capacities [32]. A super absorbent hydrogel prepared using lignin and PVA has demonstrated dye absorption capacity [33]. In another study, a bionanocomposite hydrogel based on Eggwhite and Polyvinyl alcohol, incorporated with

MMT, was found to effectively remove methylene blue dye [34]. Additionally, PVA modified with FPBA (4-formylphenylboronic acid) and TDH (tartaric acid dihydrazide) forms an ultra-fast self-healing organogel capable of absorbing organic dyes [35]. PVA/GO nano fiber film has shown increased adsorption properties for organic dyes and Cu^{2+} metal [36]. Furthermore, PVA/cellulose nanofibril (CNF) aerogels modified with methyl trichlorosilane have exhibited oil absorption capacity approximately 96 times their weight and can scavenge Pb^{2+} and Hg^{2+} [37]. Similarly, PVA/bamboo cellulose nanofibers (BCNFs) -based aerogels modified with methyl trichlorosilane have proven effective in absorbing organic solvents (hexane) and pump oil [38]. Another study has shown that PVA quaternized lignin (QL) composite can effectively remove nitrate from solutions [39]. Finally, a highly porous and ultra-low -density superhydrophobic aerogel was prepared by crosslinking PVA with cellulose nanofibril, which is capable of absorbing oils as well as solvents [40].

Considering the current challenges in purifying aquatic contamination and the need for improved properties, this study aims to prepare a polymeric organogel using Polyvinyl Alcohol (PVA) and a long-chain fatty acid (Stearic Acid). The sorption process using fatty acids has been rarely investigated. In this work, the long alkyl chain of the fatty acid is utilized to enhance the hydrophobic nature of the organogel for efficient absorption of organic solvents. The study focuses on evaluating the absorption capacity and kinetics of the organogel for organic solvents, as well as investigating its thermal, mechanical, and chemical resistance properties.

2.2 EXPERIMENTAL

2.2.1 Materials

Polyvinyl Alcohol (PVA) (MW ranging between 13,000-23,000, 98.5-99.5% hydrolysed) was purchased from Otto (Chemika-biochemika-reagents), stearic acid (SA) from Loba Chemie Pvt. Ltd and dimethyl sulfoxide (DMSO) from Merck EMPLURA® (A.R. grade) were used without any purification. Toluene-4-sulphonic acid (98%) was supplied by BDH Laboratory Supplies, Sodium hydroxide pellets from Merck EMPLURA® and absolute alcohol purchased from Helix India were of AR grade and used as received.

2.2.2 Preparation of Organogels

In a typical procedure, 0.143mmol of PVA was dissolved in 10ml of DMSO in a 100ml round bottom flask equipped with a thermometer and placed over a magnetic stirrer at 80 ºC. *p*-toluene sulphonic acid was added to the dissolved PVA solution, followed by the slow addition of stearic acid under continuous stirring for 6hour (Table1.1). The reaction was stopped on attaining a jelly-like appearance. The mixture was poured into a Petri dish and washed with sodium bicarbonate ($NaHCO_3$) solution. After washing with ethanol, the organogel was dried under reduced pressure(vacuum) at 40 ºC.

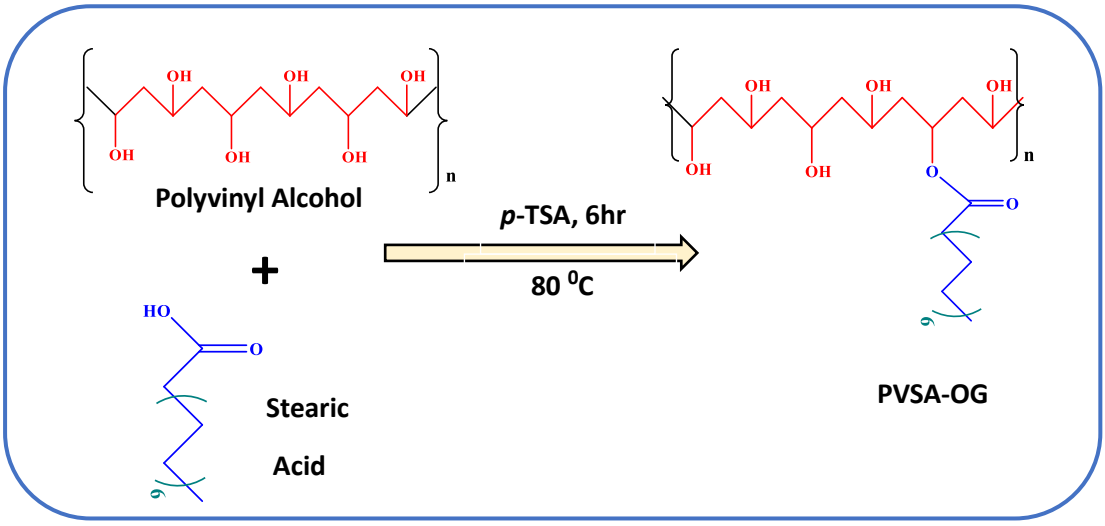

Scheme 2.1 Representation of the interaction between PVA and Stearic acid

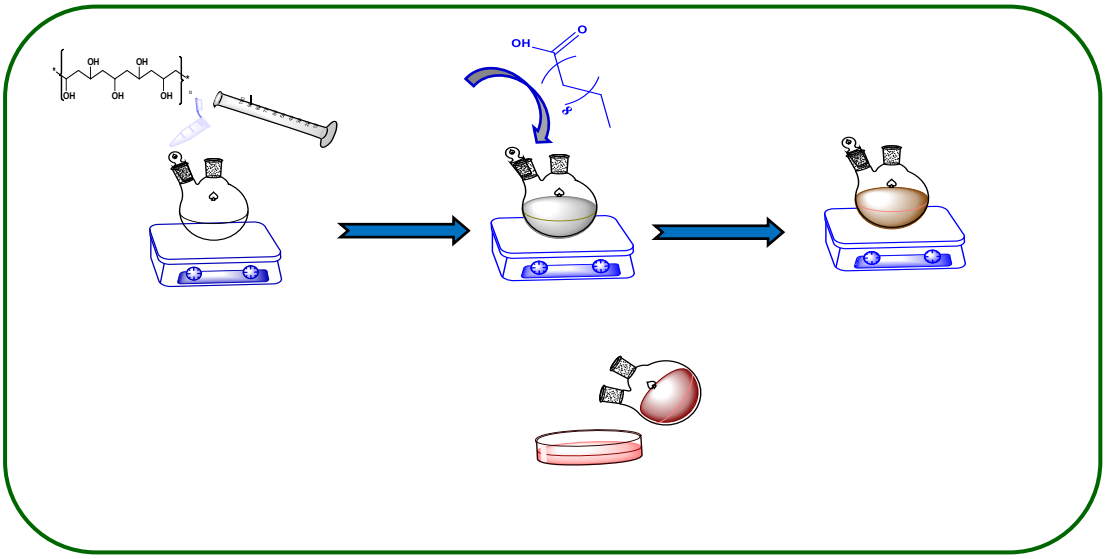

Scheme 2.2 Reaction steps involved in formation of the organogel

Table 2.1 Composition of Polyvinyl Alcohol-based Organogel

SAMPLE	PVA (mmol)	SA (mmol)	NATURE OF THE MATERIAL	CONTACT ANGLE (degree)
PVSA-OG15	0.143	15.61	Gel	51.7
PVSA-OG26	0.143	26.01	Gel	64.2
PVSA-OG39	0.143	39.02	Gel	73.9
PVSA-OG52	0.143	52.03	Gel	85.5

2.2.3 Characterization

2.2.3.1 Fourier transform infrared (FT-IR) spectroscopy analysis

FT-IR, a prominent analytical technique was used for determining the presence of functional groups in the structure of the prepared material. Functioning of FTIR depends on the interaction of infrared (IR) electromagnetic radiation with a mass of the material resulting in the absorption of a certain wavelength in that radiation. The characteristic absorption of a specific band/group arises when the transition energies between the vibrational and rotational states of the groups present in the materials fall under the infrared region. FT-IR spectra were analysed with samples on KBr pellets using Nicolet Impact-410 IR (Matison, UK) spectrometer within a frequency range of (4000-400) cm^{-1}.

2.2.3.2 Scanning electron microscopy (SEM)

SEM, a type of electron microscopy generates high resolution images of sample surface and cross-section morphologies with higher magnification. SEM uses strong electron beam under high vacuum which interacts with surface of sample, emitting secondary electron; the detection of which produces images of the surface, surface topography, composition, phase domain size, number of phases, etc. Morphological studies were obtained from JEOL SEM (JSM-6390 LV, JEOL, Japan) microscope model at an accelerating voltage of 5-15kV.

2.2.3.3 X-ray diffractometer analysis (XRD)

The spatial arrangement of all the atoms or molecules arranged in order in the sample can be detected through scanning of the sample by X-ray beams over an incidence angle of 2θ using CuKα radiation. Wide-angle X-ray diffraction patterns were recorded using a powder-XRD Diffractometer (D8 FOCUS, Bruker AXS, Germany) operating under CuKα radiation at an incidence angle of 2θ between 10º and 80º operated at a wavelength(λ) of 0.154nm.

2.2.3.4 Thermogravimetric analysis (TGA)

Thermogravimetric analysis is an essential analytical technique determining the weight/mass change of a sample against temperature under a controlled or inert atmosphere. It is used for predicting the thermal stability of the material apart from determining the weight loss of the sample due to sorption/desorption of volatiles, decomposition, or dehydration. The thermal stability of the prepared samples was studied in NETZSCH TG 209 F1 Libra® using pure nitrogen as purge gas with a flow rate of 20mL min^{-1}. The samples with mass of around 10mg were heated at 10 ºC min^{-1} with heating rate from room temperature upto 400 ºC.

2.2.3.5 Differential Scanning Colorimetry (DSC)

DSC, a thermos-analytical technique measures the difference in rate of heat flow between a sample and inert reference as a function of temperature. DSC provides phase transition temperature of a sample along with heat involved in the transition phase. The physicochemical changes involving exothermic and endothermic processes are obtained through DSC analysis. DSC measurements were performed using NETZSCH DSC 214 Polyma. Textural attributes like tensile strength was determined using a texture measuring system, Stable Micro System, TAHD-Plus (UK). Traces were recorded in alumina crucibles with pierced lids under nitrogen atmosphere at a flow rate of 20mL min^{-1}. Samples were pre-weighed before placing in alumina pan and heated from 0º to 400 ºC at a rate of 10 ºC min^{-1}.

2.2.3.6 Contact angle & Rheology

The contact angle was measured using the sessile drop method by KYOWA Interface Measurement and Analysis System (FAMAS). The deformation and flow characteristics of the gel were studied by Anton Paar RheoCompass, Model: MCR 72.

2.2.4 Absorption/Swelling analysis

The swelling absorbency of the prepared xerogel was investigated in different organic solvents. Dried samples of the organogels were immersed in a beaker containing different organic solvents to reach their equilibrium swelling at room temperature. The swelling of the gels was calculated using a standard equation (i) as reported in the literature [41]:

$$\textbf{Swelling (\%)} = {}^{W_S}/_{W_D} \times 100\% \qquad \textbf{(i)}$$

Where W_S and W_D are the weight of the swollen gels and dried gels, respectively.

2.2.5 Absorption/Swelling kinetics

The swelling kinetics was analysed using kinetic models [42]. The following kinetic equation (ii-v) describes the swelling rate of the gels.

The swelling rate for first-order kinetics

$$\frac{dQ}{dt} = k(Q_{max} - Q) \qquad \textbf{(ii)}$$

Integrating the rate of swelling for first-order kinetics, the following equation is obtained

$$\ln[Qmax / (Qmax - Q)] = k_1 t \qquad \textbf{(iii)}$$

On plotting ln(Qmax / Qmax – Q) versus time t, if a straight line is obtained, then the absorption follows first-order kinetics.

Equation (iv) expresses the second-order kinetics

$$\frac{dQ}{dt} = k_2(Q_{max} - Q)^2 \qquad \textbf{(iv)}$$

Integrating the rate of swelling for second-order kinetics, the following equation is obtained

$$\frac{t}{Q} = {}^{1}/_{k_2 Q_{max}^2} + {}^{1}/_{Q_{max}} t \qquad \textbf{(v)}$$

If the plotting of t/Q versus time t attains a straight line, then the swelling tends to follow the second-order equation.

2.2.6 Desorption kinetics

The desorption kinetics was determined after the attainment of maximum absorbency by the swollen sorbent. The retention time was calculated by determining the weight loss of the swollen sorbent as a function of time at room temperature. Dichloromethane solvent was used for the desorption kinetics of the prepared gel.

2.2.7 Reusability

The reusability of the synthesized organogel was analysed following the absorption and desorption cycles of the gel in DCM repeatedly for 7times.

2.3 RESULTS & DISCUSSION

2.3.1 Synthesis of Organogels

Organogels were synthesized using PVA and Stearic acid, keeping the ratio of PVA fixed (0.143mmol) while varying the composition of Stearic acid as 15.6mmol, 26mmol, 39mmol to 52mmol (Table2.1). Esterification reaction occurs between the hydroxyl groups of the PVA linear chain and carboxylic groups of the Stearic acid. The product is obtained in the form of a gel. The reaction is schematically presented in Scheme 2.1.

2.3.2 Characterization of Organogels

2.3.2.1 FT-IR analysis

FT-IR spectra suggested various characteristic peaks for the synthesized organogels. The broad peak at 3435.05cm^{-1} is attributed to the stretching vibration of the –OH group with strong intermolecular H-bonding, while the peak at 1437.50cm^{-1} represents the bending vibration of the hydroxyl group. The characteristic peak at 1744.44cm^{-1} and 1171.72cm^{-1} affirms the –C=O stretching and C–O stretching of the formed ester group. The carbonyl –C=O stretching vibration appeared at 1638.98cm^{-1} while 1021.3cm^{-1} frequency corresponds to –C–O–C=O acetal linkage. Absorption peaks at 2922.51cm^{-1}, 2852.21cm^{-1}, and 1464.91cm^{-1} represented the sp^3, sp^2 hybridized C–H stretching as well as C–H bending vibration. The frequency of 721.09cm^{-1} at the fingerprint region attributes to the cis-substituted C–H bending. The spectra analysis of FT-IR (Figure2.1b) confirms the esterification reaction.

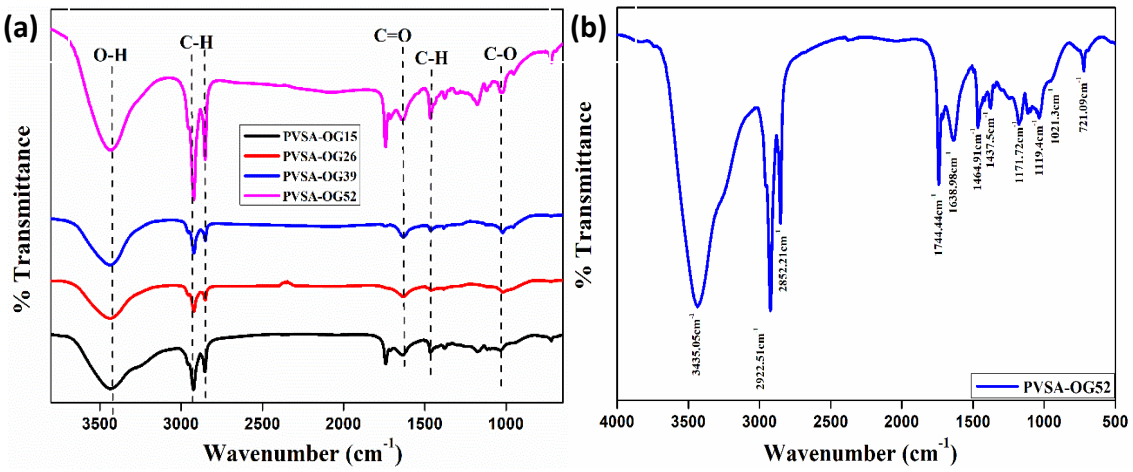

Figure 2.1 FT-IR spectra of the (a) prepared organogels PVSA-OG15, PVSA-OG26, PVSA-OG39, PVSA-OG52 (b) spectra analysis of PVSA-OG52

2.3.2.2 Morphological analysis

The morphological changes occurring on surface of PVA due to esterification was investigated using scanning electron microscope (SEM). The pristine PVA observed a uniform morphological structure (Figure 2.2a). However, the surface gradually changed and a rough morphology was attained with the formation of aggregates due to the transformation of the hydrophilic surface of PVA into a hydrophobic surface with the incorporation of stearic acid. (Figure 2.2b-e).

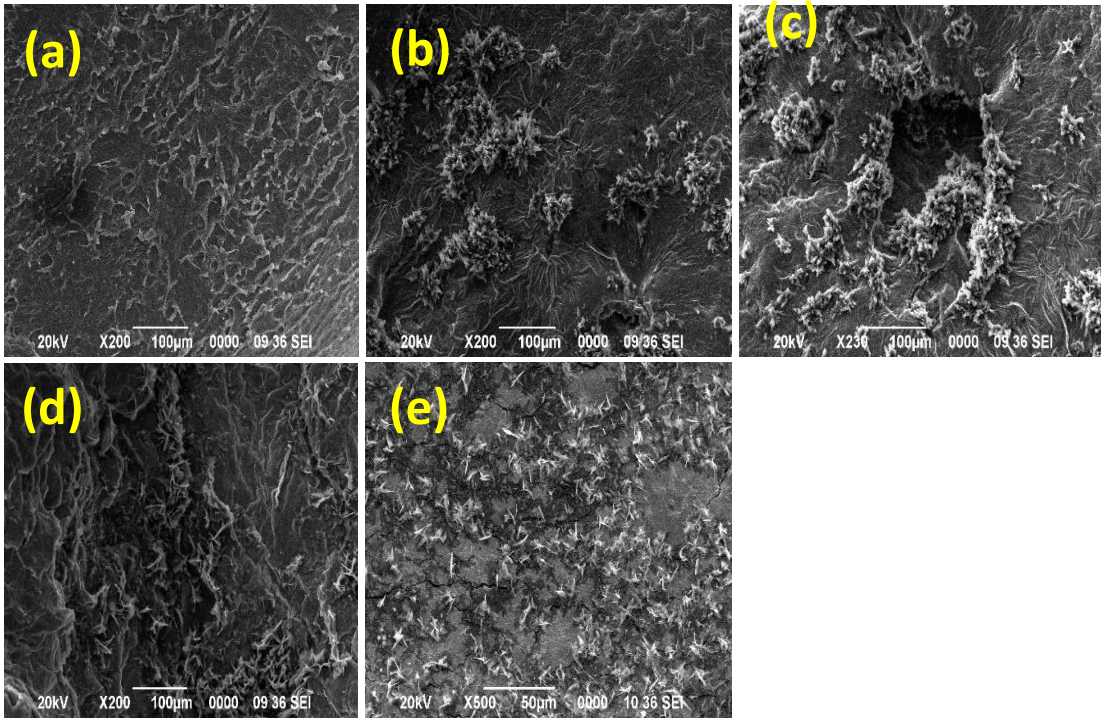

Figure 2.2 Scanning Electron Microscope Imaging of the prepared Organogels (a)PVA, (b) PVSA-OG15, (c) PVSA-OG26, (d) PVSA-OG39, (e) PVSA-OG52

2.3.2.3 XRD analysis

X-ray diffractograms for PVA and the organogels displayed three distinctive peaks at 2θ values (Figure 2.3a-c) of 19.5º with high intensity peak, 22.7º with a low intensity shoulder peak and 40.7º with a low intensity broad peak along with an interatomic spacing unit of 4.5Å, 3.9Å, 2.2Å corresponding to planes (101), (200), (102) of pristine PVA [44]. However, the base intensity of 19.5º and 40.7º with a reflection of (101, 102) seem to diminish, obtaining broad peaks with the increase in grafting of stearic acid to PVA surface. This attributes to the loss in crystallinity, emphasizing the amorphous nature of the gels.

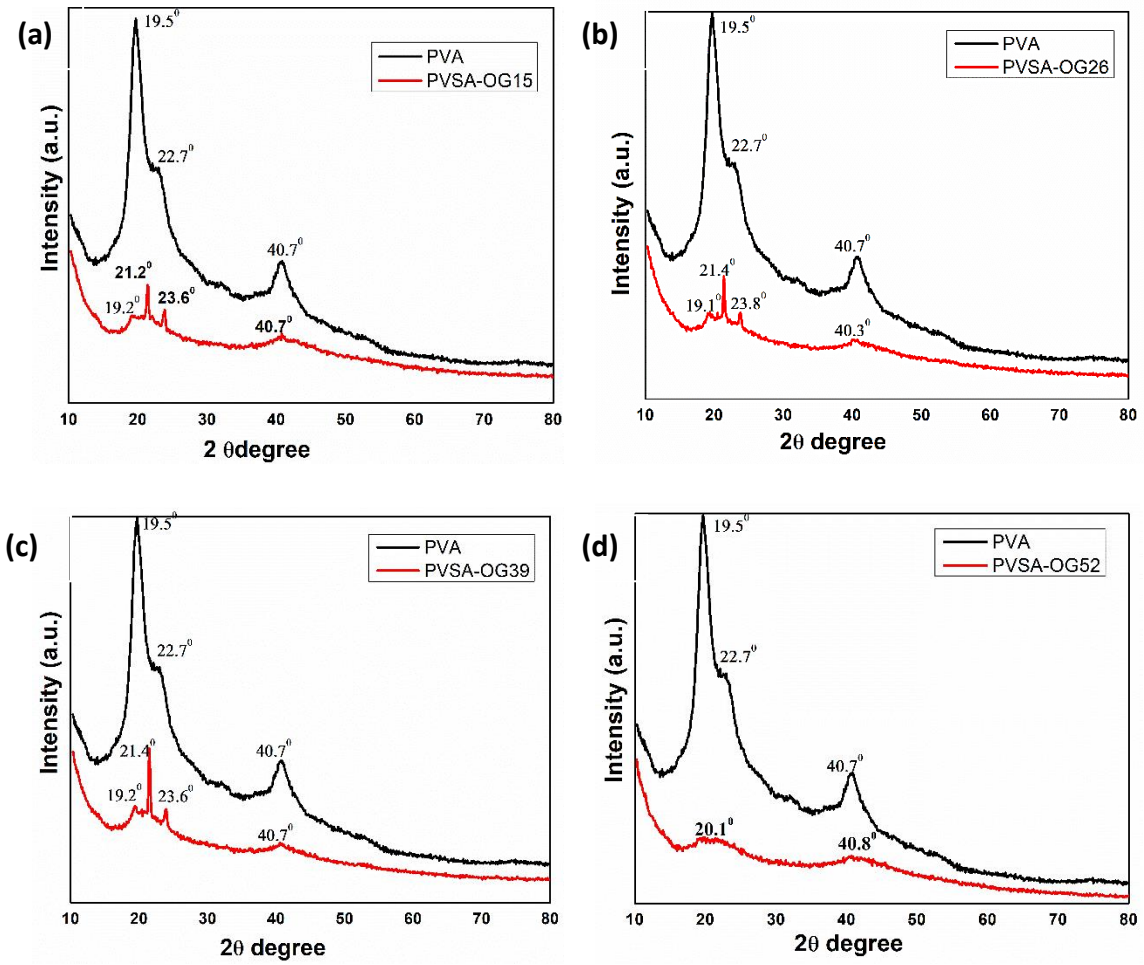

Figure 2.3 XRD spectra of the prepared organogels (a) PVSA-OG15, (b)PVSA-OG26, (c)PVSA-OG-39, (d)PVSA-OG52 with respect to PVA

2.3.2.4 TGA analysis

The major degradation temperature (T_d) was seen around 197-228 ºC for the prepared samples (Table2.2). It was observed from the TGA thermogram (Figure 2.4) that PVA observed degradation around 280 ºC. However, due to esterification with stearic acid, the degradation temperature decreased up to 228 ºC (PVSA-OG52). The initial weight loss around 100 ºC was due to loss of moisture while subsequent weight loss around 200 ºC was observed due to loss of stearic acid content from the sample. In general, degradation is initiated with the formation of free radicals at a weaker bond or the end of the chain followed by the transfer of radicals to an adjacent chain via interchain reactions. Decomposition process occurs prior in respect to PVA due to transfer of free radicals indicating increase in degradation process.

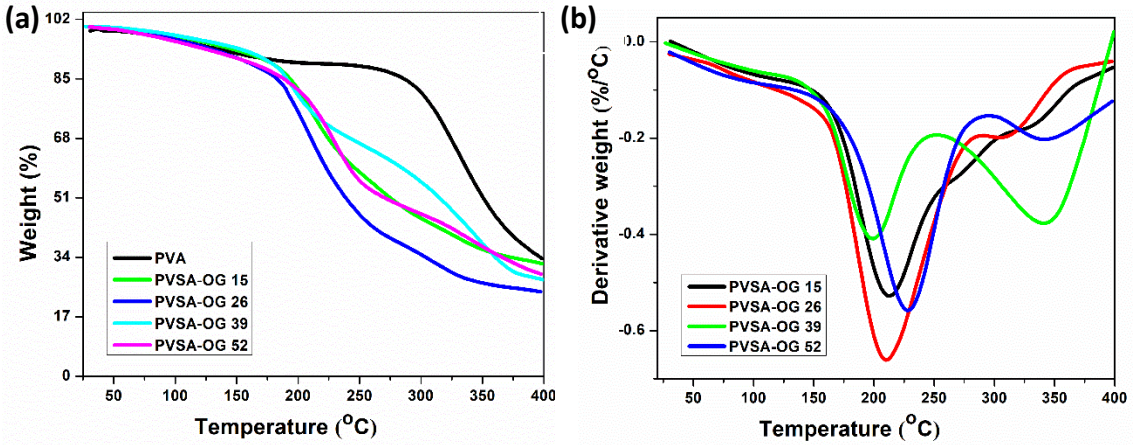

Figure 2.4 (a)TGA thermogram, (b) DTG curve of prepared organogels

The DTG curve (Figure 2.4b) indicated a major single-step weight loss primarily due to loss of solvent and functional groups followed by minor step loss depicting degradation of the PVA group with an increase in weight percent of Stearic acid. However, it has also been observed from the thermogram that degradation temperature shifts towards a higher thermal range with the increased SA ratio. Similar observations are qualitatively consistent for the decrease of value in glass transition temperature (Tg). The gel was seen to be stable up to a temperature of 170 ºC.

Table 2.2 Thermal decomposition & weight loss characteristics of the prepared organogels

SAMPLE	Major Degradation temperature (^{0}C)	Temperature (^{0}C) for weight loss at			
		30 %	45 %	60 %	80%
PVSA-OG15	207.68	398.43	298.43	243.43	203.43
PVSA-OG26	208.45	374.43	331.93	281.93	199.43
PVSA-OG39	197.95	390.19	307.69	240.19	205.19
PVSA-OG52	228.86	322.35	252.35	222.35	192.35

2.3.2.5 DSC analysis

The glass transition characteristics were obtained from differential scanning calorimetry (DSC) thermogram (Figure 2.5a). The transition value decreases significantly from 37-34 ºC with the increase in weight percent. This decrease can be explained by a slow reduction in the mobility of the polymer due to an increase in attachment of the alkyl chain of SA. An increase in melting temperature (Tm) of the organogel was observed from 208-233 ºC with the increase in weight percent. The TGA and DSC values are summarized in Table 2.3.

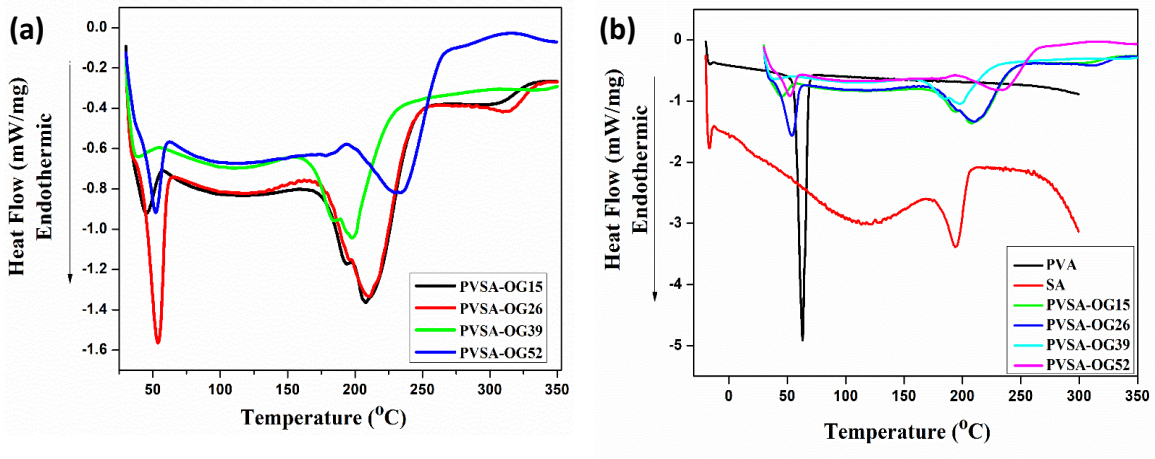

Figure 2.5 (a) DSC curves of prepared organogels (b)prepared organogels in comparison to PVA, SA

Table 2.3 Thermal decomposition characteristics of the organogels

SAMPLE	T_g(^{0}C)	T_{onset} (^{0}C)	T_{max}(^{0}C)	T_{end}(^{0}C)	ENTHALPY OF FUSION
PVSA-OG15	37	189.70	208.04	239.20	2.45
PVSA-OG26	35	184.50	210.57	237.40	2.00
PVSA-OG39	36	171.71	198.34	208.44	1.35
PVSA-OG52	34	204.41	233.68	256.48	2.41

2.3.2.6 Rheological analysis

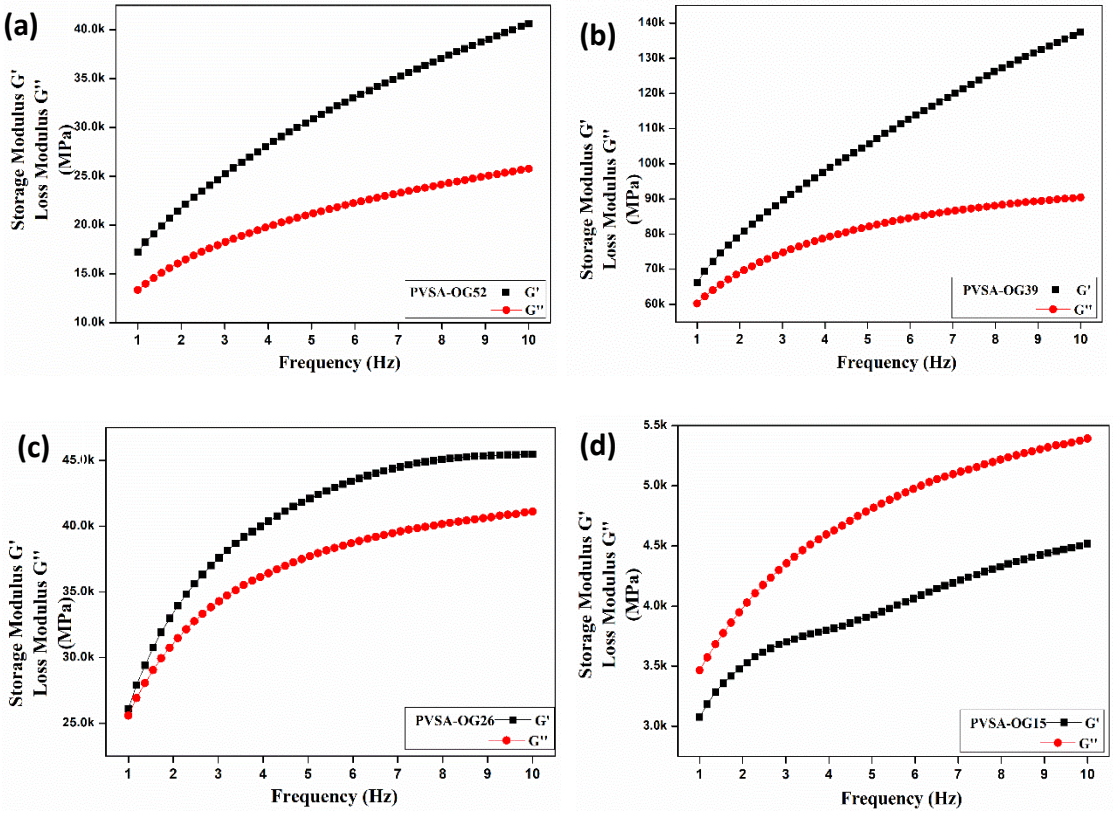

Figure 2.6 Data of storage and loss modulus from frequency sweep of the organogels (a) PVSA-OG52, (b) PVSA-OG39, (c)PVSA-OG26, (d)PVSA-OG15

Compression tests were performed to determine the rheological properties of the prepared gel. Storage modulus indicates the ability to deform against external disturbances while loss modulus determines the flow behavior under stress. The frequency sweep experiment was carried out at room temperature from 1-10 Hz at 2% strain with a 1mm distance. From Figure 2.6(a-c) elastic nature (G′>G″) of the gel can be perceived from PVSA-OG (52,39,26) while an increase in flow behavior (G″>G′) indicating viscous property was attained by PVSA-OG15 in Figure 2.6d. As the amount of SA was minimal, linkage between PVA was reduced to a larger extent exhibiting viscous property.

2.3.3 Application in solvent absorbency

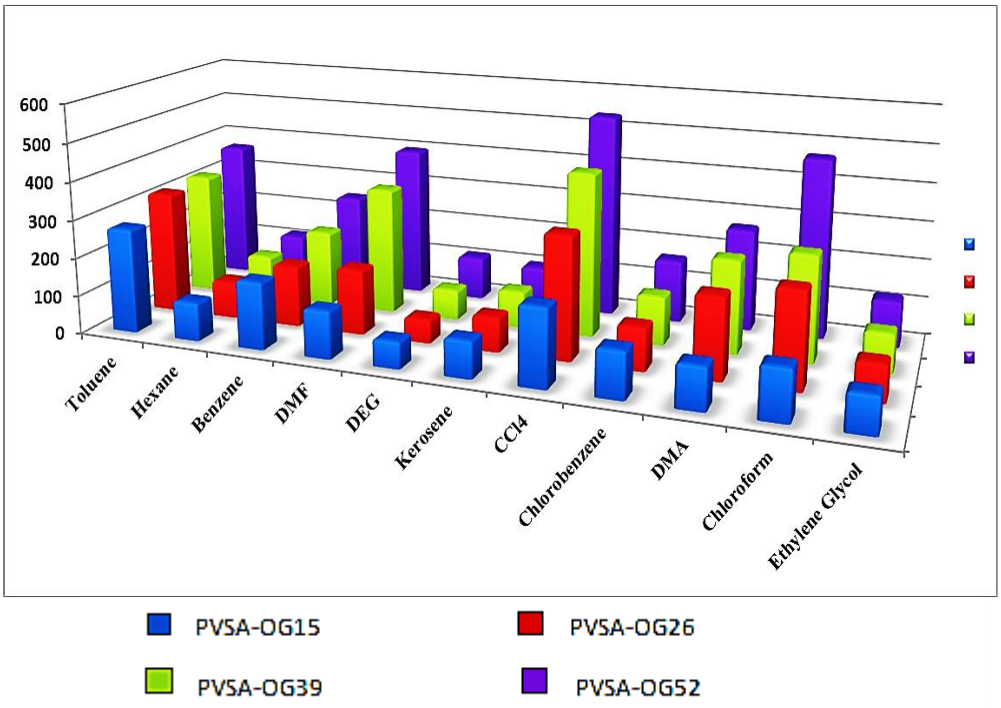

Figure 2.7: Absorption analysis of all the prepared organogels

The solvent absorbency of the prepared organogels was investigated with different solvents like Toluene, Hexane, Benzene, DMF, DEG, Kerosene, Carbon tetrachloride, Chlorobenzene, DMA, Chloroform, and Ethylene glycol, (Figure 2.7). It has been observed that maximum absorption has been achieved with PVSA-OG52 (Figure 2.7). The increase in the content of the alkyl group increases the hydrophobicity of the organogel. With the increase in weight percent of stearic acid, the contact angle of the organogel value rises from 51.7º to 85.5º, reaching the hydrophobic range (Figure 2.8).

PVSA-OG 15 **WCA= 51.7º** | **PVSA-OG 26** **WCA= 64.2º** | **PVSA-OG 39** **WCA= 73.9º** | **PVSA-OG 52** **WCA= 85.5º**

Figure 2.8 Hydrophobicity data obtained from water contact angle analysis for prepared organogels

The absorption of solvent by organogels primarily occurs through the interactions between the solvent molecules and the hydrogen bonding sites on the gelator molecules. These interactions facilitate the swelling of the gel, allowing for a greater uptake of solvents. Carbon tetrachloride, Chloroform, Toluene, and DMF exhibited more than 300% absorbency. The absorbency in carbon tetrachloride increases from 201.9% in PVSA-OG15 to 534.54%in PVSA-OG52 (Figure 2.7). The solvent absorbency of PVSA-OG52 was found to be 365.49% for Toluene, 118.53% for Hexane, 248.48% for Benzene, 398.43% for DMF, 109.46% for DEG, 104% for kerosene, 534.53% for Carbon tetrachloride, 164.13% for Chlorobenzene, 266.39% for DMA, 467.74% for Chloroform, 121.05% for Ethylene glycol respectively as observed in Figure 2.9.

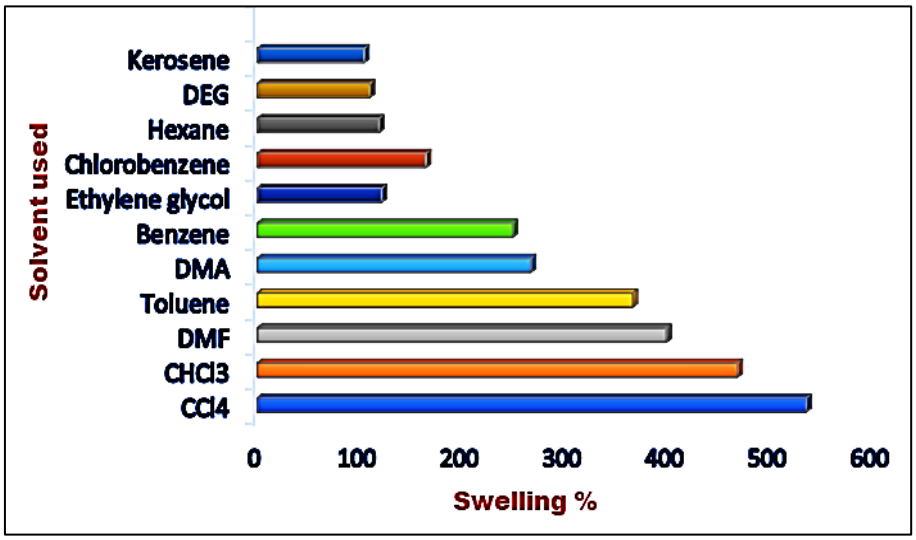

Figure 2.9 Swelling capacity of PVSA-OG52 with maximum absorbency in different organic solvents

Carbon tetrachloride showed the highest absorbency of 534.53% (Figure 2.9); this is possibly due to the matching of the polarity of carbon tetrachloride with the polymer network. Carbon tetrachloride being non-polar has zero dipole moment.

However, some solvents like ethylene glycol, Benzene, and Hexane with zero dipole moment observed the least absorbance. This is due to the molecular size of the solvent, which restricts its diffusion into the polymer network. Changes in absorbance peak were observed in the structural data of the organogel after absorption by the solvent can be viewed from the FT-IR spectra (Figure 2.10).

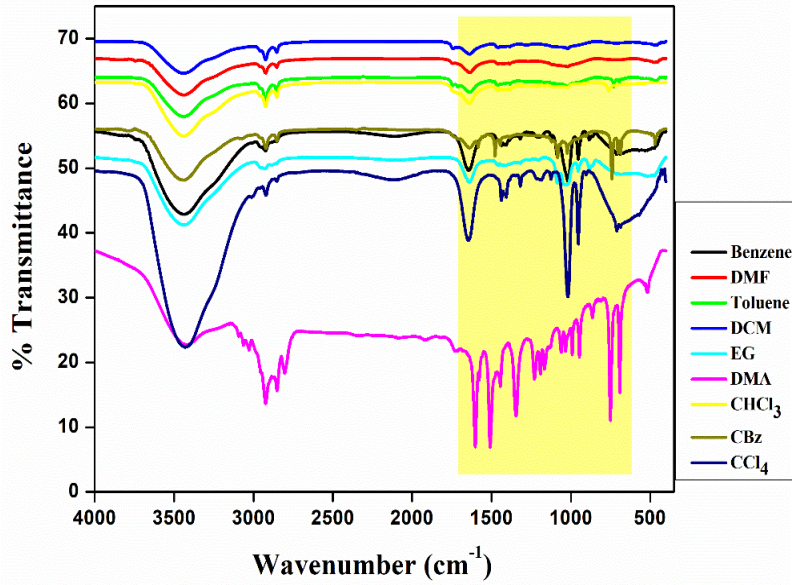

Figure 2.10 FT-IR spectra of organogel after absorption of organic solvents

2.3.4 Absorption & Desorption kinetics

The absorption kinetics of organic solvent absorption into organogels can be described with equation (iii) and equation (v). It has been found that absorption kinetics of the organogel developed a best fitted linear relationship with second-order absorption (Figure 2.11). The plot of t/Q versus time t confirms the absorption of solvents into the organogel follows second-order kinetics. The correlation coefficient suggested equivalent concurrency between actual and experimented values (Table 2.4).

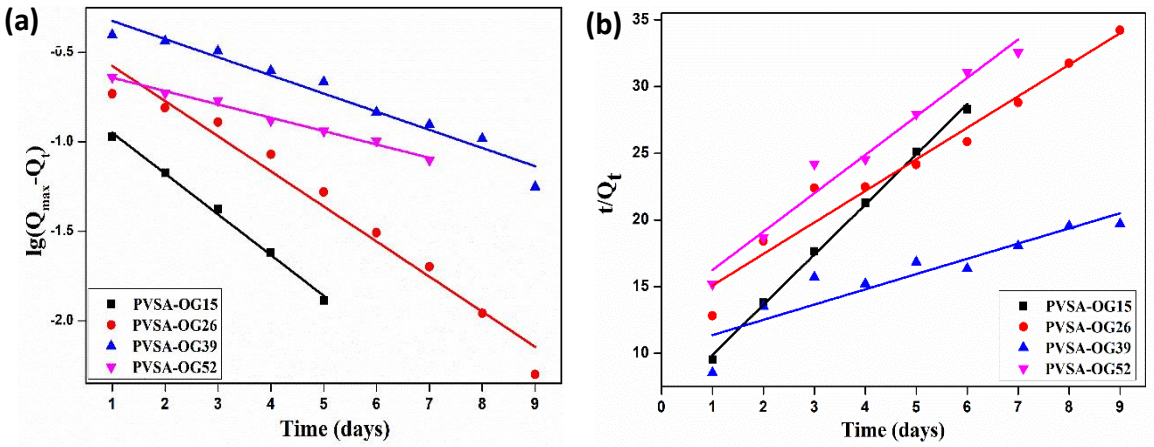

Figure 2.11 Kinetics plot for (a) first order, (b) second-order kinetics of the absorbed organogels

Table 2.4: Kinetic parameters for second-order kinetic graph of absorbed organogels

SAMPLE	$Q_{max}(gg^{-1})$	$k_2(gg^{-1}min^{-1})$	R^2 (first order)	R^2 (second order)
PVSA-OG15	266.1	1.63×10^{-4}	**0.99**	**0.99**
PVSA-OG26	423.1	0.64×10^{-4}	**0.95**	**0.96**
PVSA-OG39	875.5	0.15×10^{-4}	**0.94**	**0.87**
PVSA-OG52	347.2	0.96×10^{-4}	**0.96**	**0.98**

Desorption kinetics of the swollen organogels were studied by investigating the removal percentage of solvent DCM at different time intervals at room temperature (Figure 2.12a). It can be observed that 61%,56%,43%, and 65% of solvent can be effectively recovered from the solvent, respectively, for PVSA-OG15, PVSA-OG26, PVSA-OG39, PVSA-OG52.

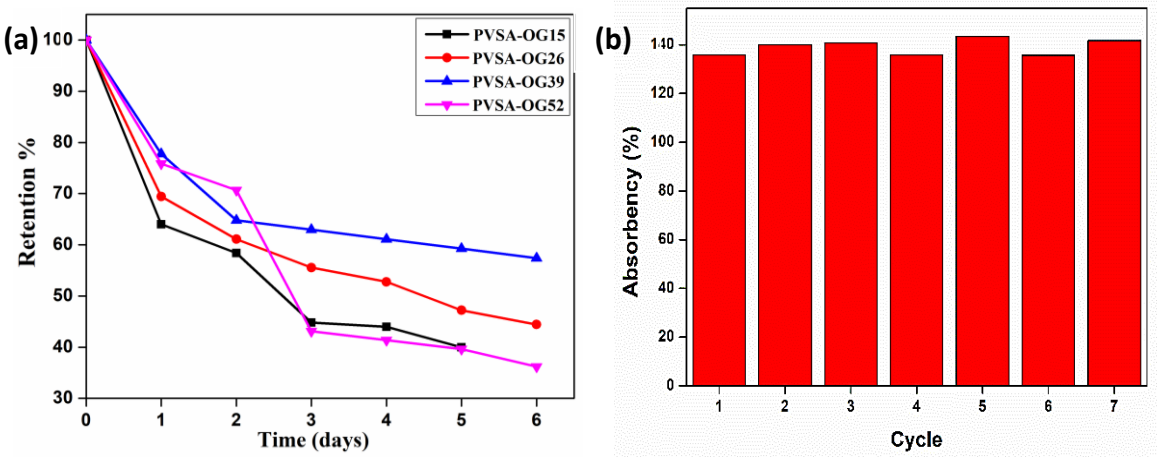

Figure 2.12 (a)Desorption kinetics graph for the prepared organogels (b)Reusability graph of PVSA-OG52 organogel in DCM

We have found absorption and desorption up to 7 cycles. The absorption capacity remains unchanged with each cycle. Figure (2.12b) displays the regeneration efficiency of the organogel with each cycle.

2.4 CONCLUSION

We have developed an organogel based on fatty acid-modified polyvinyl alcohol. The effectiveness of these organogels in absorbing various organic solvents has been investigated. Among the tested solvents, the organogel with a higher stearic acid content demonstrated the highest absorbency, specifically absorbing 534.54% of carbon tetrachloride. Notably, this is the highest absorbency observed among all the solvents studied. The organogel exhibits a predominantly hydrophobic nature, as indicated by a

contact angle of 88.5°. Interestingly, the absorbency of carbon tetrachloride, despite being a non-polar solvent, is influenced by the size of the solvents employed. It is important to conduct further studies to establish a correlation between absorbency and the structure-property relationship. The absorption of solvents by the organogel follows second-order kinetics and demonstrates favorable solvent retention and reusability properties. Consequently, the synthesized organogel exhibits promising potential as a material for the absorption of organic solvent seepage from the environment.

2.5 REFERENCES

[1] Lee, P., and Rogers, M. A. Phase-Selective Sorbent Xerogels as Reclamation Agents for Oil Spills. *Langmuir*, 29 (18): 5617–5621, 2013.

[2] Kizil, S., Karadag, K., Aydin, G. O., and Sonmez, H. B. Poly (Alkoxysilane) Reusable Organogels for Removal of Oil/Organic Solvents from Water Surface. *Journal of Environmental Management*, 149: 57–64, 2015.

[3] Fingas, M. *The Basics of Oil Spill Cleanup*, Second Edition. ISBN-13: 978-1-4200-3259-8. CRC Press Taylor & Francis Group, 1978.

[4] Chen, J., Zhang, W., Wan, Z., Li, S., Huang, T., and Fei, Y. Oil spills from global tankers: Status review and future governance. *Journal of Cleaner Production*, 227: 20-32, 2019.

[5] Aydin, G. O., and Sonmez, H. B. Hydrophobic Poly (Alkoxysilane) Organogels as Sorbent Material for Oil Spill Cleanup. *Marine Pollution Bulletin*, 96 (1–2): 155–164, 2015.

[6] Chaza, C., Sopheak, N., Mariam, H., David, D., Baghdad, O., and Moomen, B. Assessment of Pesticide Contamination in Akkar Groundwater, Northern Lebanon. *Environmental Science and Pollution Research*, 25 (15): 14302–14312, 2018.

[7] Gobelius, L., Hedlund, J., Dürig, W., Tröger, R., Lilja, K., Wiberg, K., and Ahrens, L. Per- and Polyfluoroalkyl Substances in Swedish Groundwater and Surface Water: Implications for Environmental Quality Standards and Drinking Water Guidelines. *Environmental Science & Technology*, 52 (7): 4340–4349, 2018.

[8] Busca, G., Berardinelli, S., Resini, C., and Arrighi, L. Technologies for the Removal of Phenol from Fluid Streams: A Short Review of Recent Developments. *Journal of Hazardous Materials*, 160 (2-3): 265-288, 2008.

[9] Tubić, A., Lončarski, M., Maletić, S., Jazić, J. M., Watson, M., Tričković, J., and Agbaba, J. Significance of Chlorinated Phenols Adsorption on Plastics and Bioplastics during Water Treatment. *Water*, 11 (11), 2358, 2019.

[10] Oluwasanu, A. A. Fate and Toxicity of Chlorinated Phenols of Environmental Implications: A Review. *Medicinal & Analytical Chemistry International Journal*, 2 (4), 2018.

[11] Krishnamoorthy, R., Choudhury, A. R., Jose, P. A., Suganya, K., Senthilkumar, M., Prabhakaran, J., Gopal, N. O., Choi, J., Kim, K., Anandham, R., and Sa, T. Long-Term Exposure to Azo Dyes from Textile Wastewater Causes the Abundance of Saccharibacteria Population. *Applied Sciences*, 11 (1), 379, 2021.

[12] Liu, Q. Pollution and Treatment of Dye Waste-Water. In IOP Conference Series: *Earth and Environmental Science*, 514, 052001, 2020.

[13] Ossai, I. C., Ahmed, A., Hassan, A., and Hamid, F. S. Remediation of Soil and Water Contaminated with Petroleum Hydrocarbon: A Review. *Environmental Technology & Innovation*, 17, 100526, 2020.

[14] Truskewycz, A., Gundry, T. D., Khudur, L. S., Kolobaric, A., Taha, M., Medina, A. A., Ball, A. S., and Shahsavari, E. Petroleum Hydrocarbon Contamination in Terrestrial Ecosystems—Fate and Microbial Responses. *Molecules*, 24 (18), 2019.

[15] Karpińska, J., and Kotowska, U. Removal of Organic Pollution in the Water Environment. *Water*, 11 (10), 2019.

[16] Huang, R., McPhedran, K. N., Sun, N., Ayala, P. C., El-Din, M. G. Investigation of the Impact of Organic Solvent Type and Solution PH on the Extraction Efficiency of Naphthenic Acids from Oil Sands Process-Affected Water. *Chemosphere*, 146: 472–477, 2016.

[17] Tian, M., Fang, L., Yan, X., Xiao, W., and Row, K. H. Determination of Heavy Metal Ions and Organic Pollutants in Water Samples Using Ionic Liquids and Ionic

Liquid-Modified Sorbents. *Journal of Analytical Methods in Chemistry*, 14-15: 1-19, 2019.

[18] Fallahzadeh, R. A., Khosravi, R., Dehdashti, B., Ghahramani, E., Omidi, F., Adli, A., and Miri, M. Spatial Distribution Variation and Probabilistic Risk Assessment of Exposure to Chromium in Ground Water Supplies; a Case Study in the East of Iran. *Food and Chemical Toxicology*, 115: 260–266, 2018.

[19] Kurwadkar, S. Occurrence and Distribution of Organic and Inorganic Pollutants in Groundwater. *Water Environment Research*, 91 (10): 1001–1008, 2019.

[20] Gisi, S. D., Lofrano, G., Grassi, M., and Notarnicola, M. Characteristics and Adsorption Capacities of Low-Cost Sorbents for Wastewater Treatment: A Review. *Sustainable Materials and Technologies*, 9: 10-40, 2016.

[21] Lim, J. Y. C., Goh, S. S., Liow, S. S., Xue, K., and Loh, X. J. Molecular Gel Sorbent Materials for Environmental Remediation and Wastewater Treatment. *Journal of Materials Chemistry A*, 7 (32): 18759–18791, 2019.

[22] Yati, I., Aydin, G. O., Sonmez, H. B. Cross-Linked Poly (Tetrahydrofuran) as Promising Sorbent for Organic Solvent/Oil Spill. *Journal of Hazardous Materials*, 309: 210–218, 2016.

[23] Yati, I., Karadag, K., Sonmez, H. B. Amphiphilic Poly (Ethylene Glycol) Gels and Their Swelling Features. *Polymers for Advanced Technologies*, 26 (6): 635–644, 2015.

[24] Erdem, A. Synthesis and Characterization of Polypropylene Glycol-Based Novel Organogels as Effective Materials for the Recovery of Organic Solvents. *Journal of Applied Polymer Science*, 138 (7), 2021.

[25] Sar, P., Roy, S. G., De, P., and Ghosh, S. Synthesis of Glutamic Acid Derived Organogels and Their Applications in Dye Removal from Aqueous Medium. *Macromolecular Materials and Engineering*, 305 (4), 2020.

[26] Goel, S., and Jacob, J. D-Galactose-Based Organogelator for Phase-Selective Solvent Removal and Sequestration of Cationic Dyes. *Reactive and Functional Polymers*, 157, 104766, 2020.

[27] Bidgoli, H., Mortazavi, Y., and Khodadadi, A. A. A Functionalized Nano-Structured Cellulosic Sorbent Aerogel for Oil Spill Cleanup: Synthesis and Characterization. *Journal of Hazardous Materials*, 366: 229–239, 2019.

[28] Nguyen, P. Q. P., Hoang, A. T., and Tawaha, A. R. M. S. A Study of Oil Absorbing Capacity of Cellulose-Implemented Polyurethane for the Recovery of Oil Spills. *International Journal of e-Navigation and Maritime Economy*, 9: 25-34, 2018.

[29] Krumova, M., López, D., Benavente, R., Mijangos, C., and Pereña, J. M. Effect of Crosslinking on the Mechanical and Thermal Properties of Poly (Vinyl Alcohol). *Polymer*, 41 (26): 9265-9272, 2000.

[30] Costa-Júnior, E. S., Barbosa-Stancioli, E. F., Mansur, A. A. P., Vasconcelos, W. L., and Mansur, H. S. Preparation and Characterization of Chitosan/ Poly (Vinyl Alcohol) Chemically Crosslinked Blends for Biomedical Applications. *Carbohydrate Polymers*, 76 (3): 472–481, 2009.

[31] Teodorescu, M., Bercea, M., and Morariu, S. Biomaterials of Poly (Vinyl Alcohol) and Natural Polymers. *Polymer Reviews*, 58 (2): 247–287, 2018.

[32] Yin, T., Zhang, X., Liu, X., and Wang, C. Resource Recovery of Eichhornia Crassipes as Oil Superabsorbent. *Marine Pollution Bulletin*, 118 (1–2): 267–274, 2017.

[33] Wu, L., Huang, S., Zheng, J., Qiu, Z., Lin, X., and Qin, Y. Synthesis and Characterization of Biomass Lignin-Based PVA Super-Absorbent Hydrogel. *International Journal of Biological Macromolecules*, 140: 538–545, 2019.

[34] Khadivi, H., Sirousazar, M., Chianeh, V. A., and Jalilnejad, E. Egg White/Polyvinyl Alcohol/Clay Bionanocomposite Hydrogel Adsorbents for Dye Removal. *Journal of Polymers and the Environment*, 30: 3186-3202, 2021.

[35] Ren, S., Sun, P., Wu, A., Sun, N., Sun, L., Dong, B., and Zheng, L. Ultra-Fast Self-Healing PVA Organogels Based on Dynamic Covalent Chemistry for Dye Selective Adsorption. *New Journal of Chemistry*, 43 (20): 7701–7707, 2019.

[36] He, Y., Tian, H., Xiang, A., Ma, S., Yin, D., and Rajulu, A. R. Fabrication of PVA/GO Nanofiber Films by Electrospinning: Application for the Adsorption of Cu2+ and Organic Dyes. *Journal of Polymers and the Environment*, 30 (7): 1-12, 2022.

[37] Zhai, T., Zheng, Q., Cai, Z., Xia, H., and Gong, S. Synthesis of Polyvinyl Alcohol/Cellulose Nanofibril Hybrid Aerogel Microspheres and their use as Oil/Solvent superabsorbents. *Carbohydrate Polymers*, 148: 300–308, 2016.

[38] Han, S., Yao, Q., Jin, C., Fan, B., Zheng, H., and Sun, Q. Cellulose Nanofibers from Bamboo and Their Nanocomposites with Polyvinyl Alcohol: Preparation and Characterization. *Polymer Composites*, 39 (8): 2611–2619, 2018.

[39] Li, Y., Lin, X., Zhuo, X., and Luo, X. Poly (Vinyl Alcohol)/Quaternized Lignin Composite Absorbent: Synthesis, Characterization and Application for Nitrate Adsorption. *Journal of Applied Polymer Science*, 128 (5): 2746–2752, 2013.

[40] Zheng, Q., Cai, Z., and Gong, S. Green Synthesis of Polyvinyl Alcohol (PVA)-Cellulose Nanofibril (CNF) Hybrid Aerogels and Their Use as Superabsorbents. *Journal of Materials Chemistry A*, 2 (9): 3110–3118, 2014.

[41] Thakur, V. K., Thakur, M. K., and Voicu, S. I. *Polymer Gels Perspectives and Applications Gels Horizons*: From Science to Smart Materials. ISBN 978-981-10-6079-3, 2018.

[42] Schott, H. Swelling Kinetics of Polymers. *Journal of Macromolecular Science*: *Part B*, 31 (1): 1–9, 1992.

[43] Ozcan, A., and Kandirmaz, E. A. Poly[(Vinyl Alcohol) - (Stearic Acid)] synthesis and use in lavender oil capsulation. In Proceedings of *9th International Symposium on Graphic Engineering and Design*; Faculty of Technical Sciences, pages: 189–196, 2018.

[44] Modrogan, C., Căprărescu, S., Dăncilă, A. M., Orbuleț, O. D., Grumezescu, A. M., Purcar, V., Radițoiu, V., and Fierascu, R. C. Modified Composite Based on Magnetite and Polyvinyl Alcohol: Synthesis, Characterization, and Degradation Studies of the Methyl Orange Dye from Synthetic Wastewater. *Polymers*, 13 (22), 3911, 2021.